Received: 28 March 2017 | Revised: 14 June 2017 | Accepted: 19 June 2017

DOI: 10.1002/qua.25430

FULL PAPER

WILEY International Journal of QUANTUM CHEMISTRY

Impact sensitivity of crystalline phenyl diazonium salts: A first-principles study of solid-state properties determining the phenomenon

Sergey V. Bondarchuk

Department of Chemistry and Nanomaterials Science, Bogdan Khmelnitsky Cherkasy National University, blvd, Shevchenko 81, Cherkasy 18031, Ukraine

Correspondence
Sergey V Bondarchuk, Department of Chemistry and Nanomaterials Science, Bogdan Khmelnitsky Cherkasy National University, blvd, Shevchenko 81, 18031 Cherkasy, Ukraine.
Email: bondchem@cdu.edu.ua

Funding information
Ministry of Education and Science of Ukraine, Research Fund (Grant No. 0113U001694). We thank Professor Hans Ågren (KTH, Stockholm) for the PDC supercomputer use. The computations were performed on resources provided by the Swedish National Infrastructure for Computing (SNIC) at the Parallel Computer Center (PDC) through the project "Multiphysics Modeling of Molecular Materials," SNIC 020/11-23.

Abstract

Two crystalline salts, phenyl diazonium chloride (**PDC**) and tetrafluoroborate (**PDT**), were chosen as probes for theoretical study of solid-state properties responsible for impact sensitivity since these salts differ only in the nature of anion and, hence, in the properties of solid state. In the present report, we have studied the influence of electronic structure, vibrational spectra, mechanical properties, crystal growth morphology, and the stored energy content on impact sensitivity of **PDC** and **PDT** to find the most important solid state characteristics governing this phenomenon. The band structure calculations at various external pressures indicate very different response of the band gap. Extremely sensitive **PDC** crystals acquire the metallic nature at 29 GPa (metallization point), whilst in the **PDT** crystals the complete closure of band gap occurs only at 200 GPa. Moreover, the stored energy content in **PDC** is by 1000 kJ mol^{-1} higher than that of **PDT**. Only these two properties among the calculated in the present work differ significantly in the studied crystals. The rest solid-state characteristics such as crystal packing, vibratial spectra (phonon-valence vibration energy transfer probability), elastic properties (bulk moduli) demonstrate rather close values. The influence of metallization point (GPa) as well as crystal growth morphology on impact sensitivity is discussed for the first time.

KEYWORDS
aryl diazonium salts, DFT, impact sensitivity, metallization point, stored chemical energy

1 | INTRODUCTION

Today, one of the most urgent problems of humankind is a lack of efficient energy sources. Many branches of industry, science, army, and so forth need materials enclosing huge amount of internal energy, so-called high-energy density materials (HEDMs). Modern HEDMs should satisfy very tight criteria of environmental safety.[1,2] Therefore, the most potentially favorable candidates of such "green" HEDMs are nitrogen-rich compounds including different single-bonded allotropes of nitrogen.[3–5] On explosion, these HEDMs release molecular nitrogen as a primary product, which is an environmentally friendly inert gas.

An important property of explosives is impact sensitivity (h_{50}) which determines the minimum drop height (cm) needed to initiate explosion of 50% trials. This assumes, however, that the drop weight is equal in all the cases. From this point of view it is more convenient to use the impact energy (IE) values (in J). Sensitive explosives are characterized by the IE values equal to 1–5 J.[6] Otherwise, if a 50 J impact does not cause explosion, one can classify this material as nonsensitive.[6,7]

To quantify impact sensitivity, a number of different theoretical models were proposed. Most of them are based on the analysis of various molecular features in terms of quantitative structure–property relationships (QSPR) methodology including very complex artificial neural networks.[8–18] These QSPR models, however, often include arbitrary sets of descriptors and are very sensitive to the known problem of random correlations. Conversely, the molecular properties unable to explain the differences between impact sensitivities of various polymorphic crystalline solids, for example, hexahydro-1,3,5-trinitro-1,3,5-triazine (RDX)[19,20] or octahydro-1,3,5,7-tetranitro-1,3,5,7-tetrazocine (HMX).[21]

Meanwhile, attempts were made to establish a link between impact sensitivity and the solid state properties, particularly, band gap.[22] Zhu and Xiao studied band structures of metal azides and revealed a qualitative dependence with the impact sensitivity.[23] Thus, the small gaps cause high sensitivity and subsequently small impact energy values.[22,23] The abovementioned dependence, however, cannot be applied for an arbitrary set of explosives, because divergence of the band gaps for solids is not too much as it is for impact sensitivity values. This rather can be applied for a qualitative description of impact sensitivity within a family of compounds. Additionally, at ambient pressure, band gaps are usually too large to allow an effective electron flow to conduction bands in dark conditions. According to Boltzmann distribution, in the "dark" conditions, a noticeable occupation of the conduction band at 298 K occurs only when the band gap value is lower than 1 eV.[24] Thus, the oversimplified approach based on the band gap values at ambient pressure cannot serve as a reliable criterion of impact sensitivity. It becomes clear that there are other solid state properties which affect impact sensitivity values. McNesby and Coffey proposed to use vibrational spectra to quantify impact sensitivity by means of estimation of the phonon-valence vibration energy transfer probability.[25] Zhang et al.[26] provided a description of explosives crystal composition, which allows to distinguish qualitatively sensitive and insensitive HEDMs.

Also, an important approach was developed to describe impact sensitivity as a property, which depends on the chemical energy stored in the material (Q).[27,28] This value is proportional to the crystalline enthalpies of formation ($\Delta H^0_{f(s)}$). Wu and Fried have shown that the bond dissociation energy scaled by the energy content (Q) is a promising indicator for predicting high explosive sensitivity.[27] It was found that stored energy values yield dramatic improvement with respect to simple QSPR approaches, at least for common nitroaliphatic explosives.[29] Thus, the influence of stored energy content on impact sensitivity of **PDC** and **PDT** crystals should be also checked.

From this point of view, it is interesting to study aryl diazonium salts which have the known mechanism of decomposition.[30,31] In this case, once the virtual orbitals become occupied the structure loses nitrogen generating radical species.[32,33] This process, obviously, initiate a chain reaction and subsequent explosion. Thus, we can speculate, that when empty bands become occupied structure starts to decompose; this explains the effect of band gap values.

To take into account all the aforementioned factors affecting impact sensitivity, we have chosen two crystalline aryl diazonium salts, phenyl diazonium chloride (**PDC**) and tetrafluoroborate (**PDT**), as probes whose crystal structures are well-known.[34,35] These salts strongly differ in stability:[36] **PDC** is extremely unstable with IE equal to 3 J.[7] In contrast, **PDT** has very high stability and can be safely stored and handled without special care.[37] Such unique stability is peculiar for aryl diazonium salts with another weakly nucleophilic anion, tosylate (TsO^-).[38,39] Since the studied salts consist of the same phenyl diazonium cation and differ only in the nature of the anion, the difference in impact sensitivity should be addressed solely to the properties of solid state.

Thus, in this article we have tried to understand what solid-state derived properties including electronic structure, vibrational spectra, and elasticity can be representatives of impact sensitivity. For this purpose, we have performed first-principles calculations of **PDC** and **PDT** at ambient and high external pressures.

2 | COMPUTATIONAL DETAILS

First-principles calculations presented in this work were performed within the generalized gradient approximation (GGA) using Materials Studio 7.0 suite of programs.[40] Cell relaxations, band structure (BS), and mechanical properties calculations were carried out using Cambridge Serial Total Energy Package (CASTEP) code.[41] The calculations have been performed with a norm-conserving pseudopotential (NCP) in reciprocal space which allows a correct description of the electron-core interactions. The functional due to Perdew–Burke–Ernzerhof (PBE)[42] has been utilized entirely. The electronic wave functions have been expanded in a plane wave basis set with an energy cutoff equals 600 eV (44.1 Ry). The Brillouin zone sampling was performed by means of the Monkhorst–Pack scheme using $1 \times 4 \times 2$ (**PDC**) and $1 \times 2 \times 4$ (**PDT**) k-point grids (0.05 $Å^{-1}$) during cell relaxations. The BS calculations were done using a wider energy cutoff equals 800 eV (58.8 Ry) and a denser mesh of $2 \times 5 \times 3$ (**PDC**) and $1 \times 3 \times 4$ (**PDT**) (0.04 $Å^{-1}$). The SCF tolerance has been specified to be 1×10^{-6} eV $atom^{-1}$. For GGA/PBE approach the long-range effects were taken into account entirely using the Tkatchenko–Scheffler (TS) scheme,[43] which provides reliable results for the geometry optimizations.[25]

The vibrational spectra calculations of the **PDC** and **PDT** crystals were performed using $DMol^3$ code.[44] During these calculations the Brillouin zone sampling was the same as for the BS calculations. Again, we have used PBE functional, but in this case a double numerical basis set, namely, DND was applied.[45] This includes d-functions on nonhydrogen atoms. Core electrons were treated in terms of all-electron approximation including relativistic effects. Thus, harmonic vibrational frequencies are computed by diagonalizing the mass-weighted second-derivative matrix **F**, whose elements can be expressed as the following:[44,45]

$$\mathbf{F}_{ij} = \frac{1}{\sqrt{m_i m_j}} \frac{\partial^2 E}{\partial q_i \partial q_j}, \tag{1}$$

where, q_i, q_j, m_i, and m_j are Cartesian coordinates and masses of atoms i and j, respectively. Since $DMol^3$ cannot produce the second derivatives analytically, these are calculated as finite differences of first derivatives. Thus, the second derivatives are computed numerically as in Equation 2.[44,45]

$$\frac{\partial^2 E}{\partial q_i \partial q_j} \equiv \left[\frac{\partial}{\partial q_i} E(q_j+\Delta) - \frac{\partial}{\partial q_i} E(q_j)\right]/\Delta, \tag{2}$$

where Δ is an arbitrary distance by which the equilibrium geometry is displaced.

To obtain crystal habits, the crystal graphs have been first computed using COMPASS[46] (condensed-phase optimized molecular potentials for atomistic simulation studies) forcefield within the Morphology Tools module.[40] The weakest energy at the initial step was set to be equal −0.6 kcal mol^{-1}. Thereafter, the crystal morphology has been predicted by means of the attachment energy (E_{att}) calculation, which is the energy released on attachment of a growth slice to a crystal face Equation 3.[47]

$$E_{att} = E_{latt} - E_{slice} \tag{3}$$

Herein, E_{latt} is the lattice energy of the crystal; E_{slice} is energy of a growth slice with thickness *dhkl*; thus, the growth rate is proportional to E_{att}.[47] Finally, the crystal growth was allowed along the planes with maximum Miller indices [3 3 3] using a Wulff plot.

3 | RESULTS AND DISCUSSION

3.1 | Crystal packing and electronic structure

Crystal composition of **PDC** and **PDT** is illustrated in Figure 1 and the asymmetric cells dimensions data are listed in Table 1. As it follows from Table 1, the calculated results are in a good agreement with the experimental ones. Actually, when comparing the crystal packing, one can approximately discriminate the crystals as the more and less sensitive to impact. Thus, Zhang et al.[26] outlined the crystal packing criteria for sensitive and insensitive HEDMs. These include the presence of: (i) big π-conjugated molecular structures; (ii) strong intramolecular hydrogen bonds; (iii) single-atom-layered stacking interactions.[26] According to the first two criteria, the studied probes are structurally the same. Furthermore, as one can see in Figure 1, the **PDC** and **PDT** crystals both do not possess stacking interactions. As a result, we cannot say anything about the difference in impact sensitivity of the **PDC** and **PDT** crystals on the basis of the crystal packing criteria.

To gain information about electronic properties of the studied crystals, we have performed BS calculations in terms of the high-throughput approach.[48] This assumes a standardized integration scheme for all the 24 Brillouin zones within 14 Bravais lattices.[49] Thus, for the **PDC** (space group $C222_1$) and **PDT** (space group $P2_1/a$) crystals the coordinates of high symmetry *k*-points can be expressed as in Tables 2 and 3, respectively. Note that in the case of **PDC**, which has a C-centered orthorhombic lattice, we have performed the BS calculations for the corresponding primitive lattice for which the Brillouin zone is illustrated in Figure 2. The BS and partial density of states (PDOS) plots for **PDC** and **PDT** crystals at ambient pressure are shown in Figure 3.

Indeed, according to Figure 3, **PDC** really has narrower band gap than that of **PDT**. The calculated values, however, differ only about two and a half times, 1.056 versus 2.682 eV, respectively. Such small difference does not explain why **PDC** is so sensitive and the **PCT** does not. Electronic structure of the studied crystals is also different. As it follows from Figure 3, in the case of **PDC** an indirect band gap occurs since the valence band maximum (VBM) and conduction band minimum (CBM) appear at the Γ- and X-points, respectively. In contrast, the **PDT** crystal exhibits a direct band gap where the VBM and CBM appear at the X-point. Thus, electronic structure calculations at zero external pressure do not provide a solid explanation of the difference in impact sensitivity of the studied crystalline salts.

Conversely, the impact event causes a local pressure rise, which can dramatically change electronic structure of the crystalline sample. Thus, we have optimized structures and calculated the corresponding BS of the **PDC** and **PDT** crystals. As a result, an absolutely different

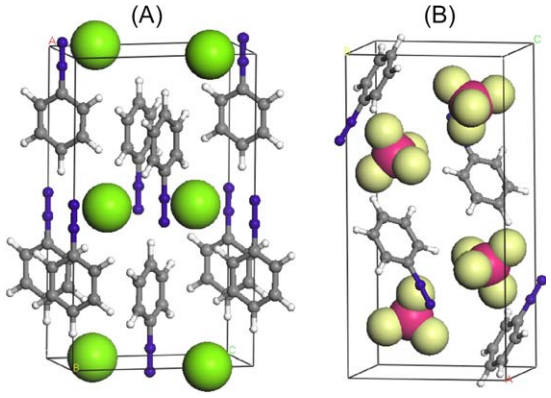

FIGURE 1 Crystal packing of **PDC** (A) and **PDT** (B)

TABLE 1 Asymmetric cell parameters for **PDC** ($C222_1$) and **PDT** ($P2_1/a$) crystals

Cell	*a* (Å)	*b* (Å)	*c* (Å)	β (°)
$\mathbf{PDC}_{exper}$	15.152	4.928	9.044	
$\mathbf{PDC}_{calcd}$	15.452	4.922	9.176	
$\mathbf{PDT}_{exper}$	17.347	8.396	5.685	92.14
$\mathbf{PDT}_{calcd}$	17.045	8.626	5.652	92.94

response of the electronic structure has been revealed in the studied crystals. It is well-known that the crystal compression accompanies with the gradual narrowing of the band gap. **PDC** has been found to be very sensitive to external pressure. When the pressure reaches 29 GPa, the complete closure of band gap occurs. Thus, electronic structure of the crystal acquires the metallic nature. We have called this pressure value as the metallization point (Figure 4A). All the intermediate values of lattice parameters for the **PDC** and **PDT** crystals at different pressures are listed in Table S1 and the corresponding BS plots are illustrated in Figures S1 and S2 in the Supporting Information.

When a molecular crystal (insulator) acquires the metallic nature, a barrierless electronic flow from the valence to conduction band takes place. The conduction band includes molecular orbitals which generally have antibonding character with respect to most bonds; therefore, their effective occupation leads to breaking of the bonds and the corresponding free radical formation. Thereafter, these radicals easily trigger the decomposition reaction, which often have chain mechanism and accompanies with an explosion. In the case of aryl diazonium salts, occupation of the lowest unoccupied molecular orbital (LUMO) leads to a subsequent loss of molecular nitrogen.[30–33] This means that in the case of aryl diazonium salts the trigger bond is the C—N bond. Since in this study we consider the same diazonium cation, the trigger bond energy is identical in terms of the molecular calculations. Thus, responsibility for the different impact sensitivity is shifted solely to the solid state properties. Hence, the metallization point becomes a crucial factor which can provide quantification of the impact sensitivity.

In the case of **PDT**, electronic system is much resistant to the lattice dimensions changes (Figure 4A). The band gap energy decreases gradually up to 200 GPa until the metallization point appears. It is interesting that in the case of **PDC** crystal, the pressure dependence of the lattice volume (VP curve) consists of two linear regions (Figure 4B). Projection of the crossing point of the corresponding tangent lines with respect to the *x* axis indicates the metallization point. The VP curve of **PDT** crystal has a similar shape, but the corresponding metallization point cannot be found using the abovementioned method; crossing of the tangent lines occurs at about 50 GPa. Since the search for metallization point is a computationally expensive task, the applicability of the scheme described above deserves a further detailed study.

The **PDT** crystals demonstrate intrinsic gap until organic moieties remain uniform. Only when extremely compression is applied (200 GPa) the organic system destroys and transforms into an amorphous matter (Figure 5).

It is worthwhile noting that such extremely high pressures are scarcely being achieved when a pure hydrostatic compression is considered under an impact event. In this case, one needs to consider an impact event at microscopic level. In this case, the hammer surface is not flat and has irregularities with surface protrusions of different size. Let's call them "contact zones." The area of a contact zone tip is obviously extremely small; therefore, the pressure formed on penetration of the tip into an explosive sample is expected to be extremely high. For example, if the tip area is 100 μm[2] and the hammer weight is 2.5 kg, a free fall from 10 cm yields the pressure rise up to 24.5 GPa and when the height is 100 cm the pressure will be 245.3 GPa.

Meanwhile, since polycrystalline samples consist of randomly distributed single crystals, the local compression causes energy redistribution uniformly toward all directions, which can be an analogue of isotropic (hydrostatic) compression. Thus, one can assume that the application of isotropic compression during the cell relaxations is justified.

TABLE 2 Definition of high symmetry *k*-points in C-centered orthorhombic $a < b$ lattice (ORCC)

k	$\times k_A$	$\times k_B$	$\times k_C$	*k*	$\times k_A$	$\times k_B$	$\times k_C$
Γ	0	0	0	*T*	−1/2	1/2	1/2
A	ζ[a]	ζ	1/2	*X*	ζ	ζ	0
A_1	−ζ	1 − ζ	1/2	X_1	−ζ	1 − ζ	0
R	0	1/2	1/2	*Y*	−1/2	1/2	0
S	0	1/2	0	*Z*	0	0	1/2

[a]$\zeta = (1 + a^2/b^2)/4$.

TABLE 3 Definition of high symmetry *k*-points in monoclinic (MCL) lattice

k	$\times k_A$	$\times k_B$	$\times k_C$	*k*	$\times k_A$	$\times k_B$	$\times k_C$
Γ	0	0	0	M_1	1/2	1−η	ν
A	1/2	1/2	0	*X*	0	1/2	0
C	0	1/2	1/2	*Y*	0	0	1/2
D	1/2	0	1/2	*H*	0	η	1−ν
H_1	0	1−η[a]	ν[b]	*Z*	1/2	0	0
M	1/2	η	1−ν	*E*	1/2	1/2	1/2

[a] $\eta=(1-b\cos\alpha/c)/(2\sin^2\alpha)$.
[b] $\nu=1/2-\eta c\cos\alpha/b$.

3.2 | Crystalline vibrational spectra

An interesting approach for quantification of the impact sensitivity was developed by McNesby and Coffey.[24] They proposed that a crucial stage in initiation of explosion is the transformation of the mechanical impact energy into phonon vibration and then into the valence vibrations. Energy evolution from phonon vibrational manifold to valence vibrational manifold proceeds via the interaction of overtones of the phonon fundamentals and the valence vibrations fundamentals.[24] Such energy transfer has a probabilistic character since it depends on the both phonon and valence vibrational fundamentals. To estimate the relative rate of the energy transfer one should first select the boundaries of the phonon and valence vibrational manifold; in the original paper these are the following 0–250 and 400–700 cm^{-1}, respectively. Thereafter, the phonon overtones should be calculated with the energy cutoff equal to the upper limit of the valence vibrational manifold (700 cm^{-1}). Once the phonon overtones are known, the difference between each of them and the valence vibrational fundamentals should be calculated.

Obviously, the greater the energies mismatch, the lower the rate of energy transfer. Usually, if the energy difference lies within the range ± 10 cm^{-1} this is a strong interaction which corresponds to a high rate, then the rate decreases rapidly. Thus, one needs to scale all the obtained differences by a cost function. McNesby and Coffey proposed to use $\mathrm{sech}^2(\Delta E/kT)$ in accord with the kinetic theory of gases.[24] Thus, impact sensitivity will be inversely proportional to the sum of scaled squares of hyperbolic secants of the obtained energy differences.

Actually, this procedure is very complex technically since one need to build and handle with extremely big arrays of data. To overcome this difficulty, we have developed a specialized utility FREQANALYZER using PascalABC.NET programming language. This allows specifying custom defined boundaries of the both phonon and valence vibrational manifolds. As a result, the sum of scaled squares of hyperbolic secants (Ω) is printed according to Equation 4.

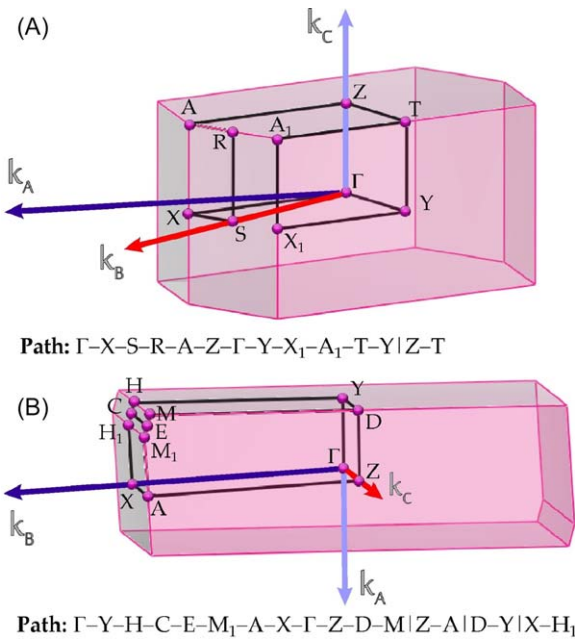

FIGURE 2 The Brillouin zone integration scheme for the **PDC** (A) and **PDT** (B) crystals along with the corresponding *k*-path within the high-throughput approximation

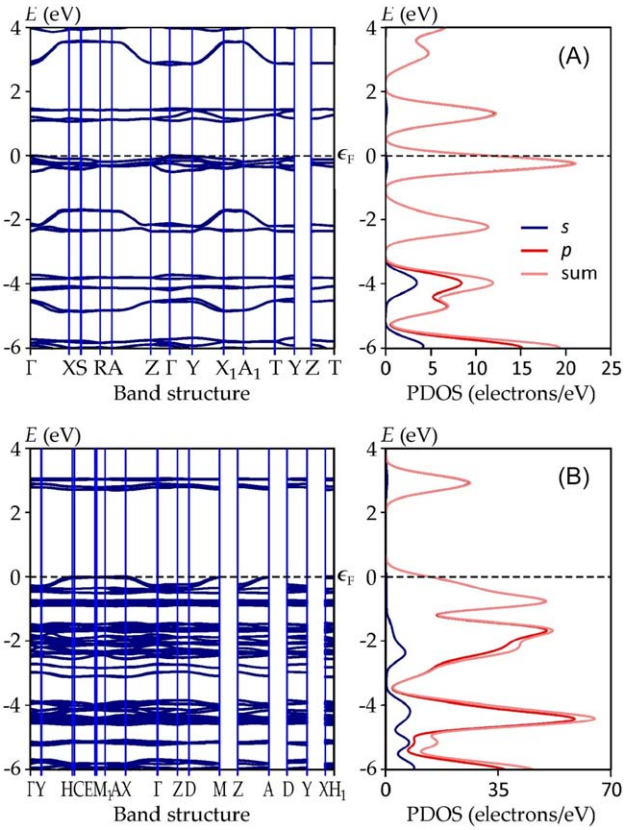

FIGURE 3 Band structure and partial density of states (PDOS) for **PDC** (A) and **PDT** (B) crystals

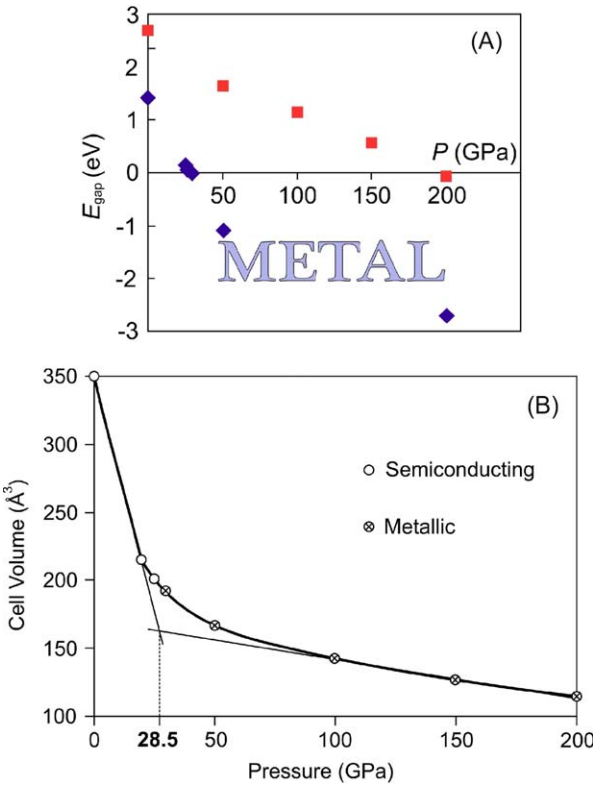

FIGURE 4 Pressure dependence of the: band gap values of **PDC** (◆) and **PDT** (■) crystals (A); **PDC** crystal volumes (B)

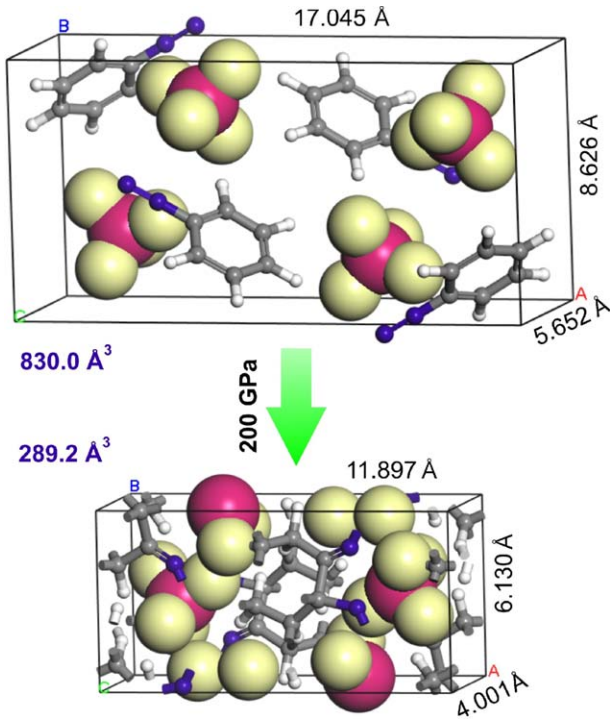

FIGURE 5 Geometry transformations in the **PDT** crystal on applied a 200 GPa hydrostatic pressure

$$\Omega = \sum_{val} \sum_{phon} \mathrm{sech}^2(\nu_{val} - \nu_{phon}), \tag{4}$$

where ν_{phon} are the frequencies of overtones and fundamentals of the specified phonons; ν_{val} are the frequencies of specified valence vibrational fundamentals. Along with this result, FREQANALYZER also prints intermediate information such as overtones which are grouped so that these data can be easily imported to any chart building tools. Also, the values of the calculated energy differences and its number are printed in the output file.

Thus, we have calculated the vibrational frequencies of the **PDC** and **PDT** crystals at the Γ-point using DMol^3 code. The numerical data are collected in Tables 4 and 5. The vibrational spectra consist of 81 and 213 normal modes for **PDC** and **PDT** crystals, respectively. Compared to our

TABLE 4 The calculated vibrational frequencies (cm^{-1}) of the crystalline **PDC**

Mode	ν	Mode	ν	Mode	ν	Mode	ν	Mode	ν	Mode	ν
1	13	15	120	29	520	43	984	57	1187	71	2284
2	37	16	125	30	622	44	985	58	1315	72	2976
3	41	17	133	31	623	45	987	59	1319	73	2978
4	46	18	153	32	672	46	1009	60	1391	74	2991
5	68	19	155	33	676	47	1011	61	1391	75	2991
6	76	20	365	34	753	48	1033	62	1449	76	3098
7	78	21	370	35	758	49	1034	63	1451	77	3098
8	90	22	402	36	774	50	1085	64	1462	78	3110
9	92	23	409	37	776	51	1094	65	1464	79	3110
10	95	24	457	38	837	52	1145	66	1575	80	3116
11	103	25	458	39	852	53	1148	67	1577	81	3116
12	107	26	511	40	959	54	1170	68	1596		
13	113	27	513	41	963	55	1172	69	1596		
14	118	28	516	42	973	56	1181	70	2277		

TABLE 5 The calculated vibrational frequencies (cm^{-1}) of the crystalline **PDT**

Mode	*v*	Mode	*v*	Mode	*v*	Mode	*v*	Mode	*v*	Mode	*v*
1	20	37	113	73	461	109	748	145	1037	181	1473
2	26	38	116	74	484	110	763	146	1048	182	1582
3	30	39	118	75	484	111	763	147	1049	183	1582
4	30	40	129	76	484	112	763	148	1050	184	1583
5	34	41	130	77	484	113	764	149	1072	185	1583
6	36	42	139	78	487	114	844	150	1098	186	1595
7	41	43	139	79	488	115	846	151	1098	187	1596
8	42	44	147	80	489	116	848	152	1099	188	1596
9	42	45	147	81	489	117	850	153	1100	189	1599
10	44	46	187	82	495	118	935	154	1129	190	2284
11	53	47	189	83	495	119	935	155	1132	191	2288
12	55	48	189	84	495	120	936	156	1133	192	2289
13	59	49	191	85	495	121	936	157	1139	193	2290
14	60	50	193	86	542	122	983	158	1163	194	3134
15	63	51	196	87	542	123	984	159	1163	195	3134
16	63	52	197	88	542	124	985	160	1164	196	3134
17	66	53	198	89	542	125	987	161	1164	197	3135
18	66	54	324	90	562	126	988	162	1186	198	3148
19	66	55	324	91	562	127	990	163	1187	199	3148
20	68	56	324	92	562	128	990	164	1190	200	3150
21	69	57	324	93	562	129	991	165	1190	201	3150
22	72	58	334	94	619	130	992	166	1317	202	3173
23	74	59	334	95	619	131	993	167	1318	203	3173
24	75	60	334	96	619	132	995	168	1319	204	3173
25	78	61	335	97	619	133	996	169	1320	205	3174
26	81	62	388	98	661	134	1005	170	1390	206	3183
27	85	63	388	99	662	135	1007	171	1390	207	3183
28	86	64	392	100	663	136	1009	172	1390	208	3183
29	87	65	394	101	663	137	1012	173	1390	209	3185
30	92	66	426	102	724	138	1019	174	1447	210	3187
31	94	67	427	103	724	139	1020	175	1447	211	3187
32	95	68	429	104	724	140	1022	176	1447	212	3188
33	100	69	429	105	724	141	1023	177	1447	213	3188
34	102	70	457	106	741	142	1023	178	1472		
35	106	71	459	107	743	143	1025	179	1472		
36	106	72	460	108	748	144	1032	180	1473		

previous results on the structure and vibrational spectra of aryl diazonium cations,[32] the data of vibrational spectra calculations obtained in the presented work are much closer to the known experimental frequencies. The results of previous molecular calculations of phenyl diazonium cation using the DFT(B3LYP)/6–31G(d,p) approach along with the presented first-principles calculations of the **PDC** and **PDT** crystals and the corresponding experimental data are gathered in Table S2 in the Supporting Information.

TABLE 6 The energy transfer probability values (Ω) for different vibrational manifold boundaries (cm^{-1}) using **PDT** as a reference

Range	400–700		400–1500		251–700		251–1500		251–3500	
Crystal	PDC	PDT	PDC	PDT	PDC	PDT	PDC	PDT	PDC	PDT
Ω	43.9480	30.9938	187.3579	180.7502	57.7993	44.9551	201.2044	194.7115	284.3802	248.0134

As it follows from Table S2, Supporting Information, the N≡N and C—N bond lengths are better reproduced using the molecular approach. In contrast, the calculated N≡N and C—N valence vibration frequencies are much closer to the experiment in the case of the crystal approximations. Thus, the DFT(B3LYP)/6–31G(d,p) approach overestimates the ν(N≡N) by 51 cm^{-1}, while the GGA/PBE/DND approach underestimates this value only by 10 cm^{-1} (Table S2, Supporting Information). We should stress that the C—N bond lengths is longer and vibtational frequency is lower for the **PDT** crystal indicating the weaker bond. Actually, this circumstance does not make **PDT** less stable than **PDC**; therefore, we can conclude that a simple approach based on the trigger bond energy approximation cannot be applied for the studied crystalline salts. Actually, the effect of the anion on structural parameters and vibrational frequencies in the C—C≡N moiety is known.[50]

The analysis of vibrational spectra of the studied salts using FreqAnalyzer utility with different boundaries of the valence vibrational manifold produced the values of Ω which are listed in Table 6. To compare the Ω values for **PDC** and **PDT** saltsobtained using FREQANALYZER, one should select a reference structure. The Ω values in Table 6 correspond to the choice of **PDT** as the reference. This means that the obtained Ω value for **PDC** should be multiplied by the factor of (N^2_{PDT}/N^2_{PDC}), where N_{PDC} and N_{PDT} are the number of normal modes in the vibrational spectra of **PDC** and **PDT**, respectively. The nonscaled Ω values for **PDC** are listed in Table S3 in the Supporting Information. As one can see in Table 6, the probability values Ω are slightly higher for **PDC** with any valence vibrational manifold boundaries; this indicates the **PDC** salt as more sensitive to impact. Conversely, the difference between, Ω values for the studied salts are not enough to explain such a big difference in impact sensitivity. Obviously, this effect has a minor character compared to the influence of metallization point. Finally, the diagram of phonon overtones together with the corresponding valence vibrational fundamentals produced by FREQANALYZER is illustrated in Figure S3 in the Supporting Information.

3.3 | Elastic properties, crystal morphology, and heats of formation

To compare mechanical properties of the studied crystalline salts, we have calculated the corresponding elasticity parameters. **PDC** belongs to the orthorhombic crystal system (space group $C222_1$) of the Laue class *mmm* and has 9 independent elastic constants.[51] At the same time, **PDT** belongs to the monoclinic crystal system (space group $P2_1/a$) of the Laue class 2/*m* and has 13 independent elastic constants.[51] The numerical values of the elastic stiffness constants C_{ij} are listed in Table 7; the Young moduli as well as the Poisson ratios are presented in Table 8.

As we have mentioned above, an important property, which significantly differs for the **PDC** and **PDT** crystals is the metallization point. Since this point reflects the pressure value, which corresponds to the band gap decrease down to zero, it has a similar meaning with bulk modulus (*B*) or compressibility (β) of a crystal. According to our present results, the calculated *B* values are the following 8.11 and 9.00 GPa for **PDC** and **PDT**, respectively. Remarkably, this result falls into the general line of the proposed hypothesis. Indeed, the more soft **PDC** crystal compresses easier and,

TABLE 7 The calculated elastic stiffness constants C_{ij} (GPa) for the studied aryl diazonium salts

PDC	***j* = 1**	***j* = 2**	***j* = 3**	***j* = 4**	***j* = 5**	***j* = 6**
i = 1	18.37	7.37	8.54	0.00	0.00	−3.28
i = 2	7.37	7.74	7.92	0.00	0.00	0.84
i = 3	8.54	7.92	9.12	0.00	0.00	−0.17
i = 4	0.00	0.00	0.00	3.91	1.11	0.00
i = 5	0.00	0.00	0.00	1.11	3.48	0.00
i = 6	−3.28	0.84	−0.17	0.00	0.00	0.24
PDT	*j* = 1	*j* = 2	*j* = 3	*j* = 4	*j* = 5	*j* = 6
i = 1	16.81	5.95	8.40	0.00	−1.52	0.00
i = 2	5.95	11.69	7.57	0.00	−0.33	0.00
i = 3	8.40	7.57	11.82	0.00	−0.58	0.00
i = 4	0.00	0.00	0.00	4.71	0.00	0.55
i = 5	−1.52	−0.33	−0.58	0.00	4.24	0.00
i = 6	0.00	0.00	0.00	0.55	0.00	3.95

TABLE 8 Young Modulus (E, GPa) and Poisson Ratios (v) for the studied diazonium crystals

Axis	E (GPa)	Poisson ratios (v)			
PDC					
x	20.8905	E_{xy}	−3.9822	E_{xz}	4.4586
y	2.2123	E_{yx}	−0.4217	E_{yz}	1.2375
z	1.2694	E_{zx}	0.2709	E_{zy}	0.7100
PDT					
x	10.4997	E_{xy}	0.0850	E_{xz}	0.6433
y	6.8094	E_{yx}	0.0551	E_{yz}	0.6025
z	5.4162	E_{zx}	0.3318	E_{zy}	0.4792

hence, the metallization point occurs faster. Conversely, the obtained close values of bulk moduli unable to explain such a big difference in the band gap closure rate. Obviously, under compression, a structural rearrangement within the asymmetric cell takes place; therefore, these two functions, $\partial V/\partial P$ and $\partial E_{gap}/\partial P$, can have different slopes. As a result, one cannot use bulk moduli to estimate the position of the metallization point. However, these can provide a crude qualitative description of the relative impact sensitivity.

It is interesting to consider the influence of the crystal growth morphology on impact sensitivity. Obviously, most of the HEDM, which are undergone by the drop weight test are polycrystalline samples. This means that the crystal habit can affect the impact sensitivity. Indeed, when a weight is dropped on the sample surface, the impact energy is transferred to the surface crystals and subsequently to the inner crystals via the contact points between them. From this viewpoint, if polycrystals in the sample are loosely packed, some part of the impact energy is spent on consolidation of polycrystals. As a result, an effective compression of polycrystals is reached at higher impact energies and, hence, at higher drop heights.

It is clear that no consolidation is expected when the crystal shape is spherical. Thus, the more the crystal habit deviates from the ideal spherical shape, the less sensitive sample is expected. To quantify such deviation of the crystal habit, we have applied the values of sphericity (Ψ), which can be expressed as the following Equation 5.

$$\Psi = \frac{S_{cryst}}{6^{2/3} V_{cryst}^{2/3} \pi^{1/3}}, \tag{5}$$

where S_{cryst} and V_{cryst} are the surface and volume of the crystal. The Ψ value determines how much the surface-volume ratio in a crystal differs from that in a sphere of the same volume.

To check this supposition, we have calculated the crystal growth morphology for the **PDC** and **PDT** crystals. The obtained crystal habits together with the corresponding Ψ values are illustrated in Figure 6. As one can see in Figure 6, the **PDC** crystals are somewhat closer to spherical shape than **PDT**. Again, this difference is rather small to provide a crucial influence on impact sensitivity, but in combination with other factors (metallization point, bulk modulus, vibratioal spectra structure) this can contribute to the value of impact sensitivity of a polycrystalline sample. Finally, since the drop weight test is usually undertaken for polycrystalline samples, the calculation approach assuming the use of isotropic compression is reasonable. Anisotropic impact sensitivity can be possible only when manipulations are carried out with a single crystal.[52]

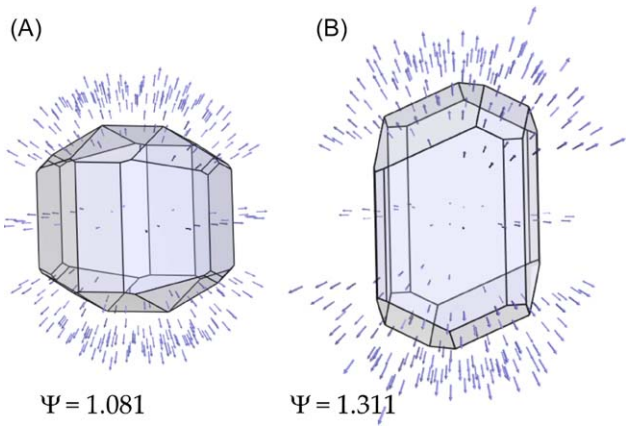

FIGURE 6 Crystal habits of the **PDC** (A) and **PDT** (B) together with the corresponding Ψ values

Finally, we have checked the relative amount of the stored energy in **PDC** and **PDT**. To perform these calculations one need to obtain the solid-state heat of formation ($\Delta H^0_{f(s)}$). Different methods for the calculation of heat of formation can be found in the literature. These include isodesmic (isogyric) reactions, atom equivalent method, and so forth. The values obtained this way are the gas-phase heats of formation which should be then transformed to the solid-state values. In this article, we have applied the following approximation:[53]

$$\Delta H^0_{f(s)} = \Delta H^0_{f(g)} - \Delta H_{\text{sub}}, \tag{6}$$

where $\Delta H^0_{f(g)}$ and ΔH_{sub} are the gas-phase enthalpy of formation and sublimation, respectively. These can be expressed using Equations 7 and 8.[53]

$$\Delta H_{\text{sub}}(T) = -E_{\text{lat}} - 2RT \tag{7}$$

$$E_{\text{lat}} = \frac{E_S}{Z} - E_g. \tag{8}$$

Herein, E_{lat} is the lattice energy obtained using the energy of the crystal (E_S) and a formula unit in the gas-phase (E_g); Z is the number of formula units per asymmetric cell.[53] Since we want to compare $\Delta H^0_{f(s)}$ for **PDC** and **PDT**, which have the same cation, the situation can be simplified. Thus, we no need to calculate $\Delta H^0_{f(s)}$ values explicitly, but can use only the difference between them.

Taking into account Equations 6–8, after transformations we obtain the following expression:

$$\Delta\Delta H^0_{f(s)} = \Delta H^0_{f(g)Cl^-} - \Delta H^0_{f(g)BF_4^-} - E_{Cl^-} + E_{BF_4^-} + \frac{1}{n}E_{PDC} - \frac{1}{m}E_{PDT} \tag{9}$$

Herein, $\Delta H^0_{f(g)Cl^-}$ and $\Delta H^0_{f(g)BF_4^-}$ are the gas-phase heats of formation of the chloride and tetrafluoroborate anions; E_{Cl^-} and $E_{BF_4^-}$ are the total energies of these ions in vacuum; E_{PDC} and E_{PDT} are the total energies of an asymmetric cell for **PDC** and **PDT**, respectively; n and m are the numbers of formula units per asymmetric cell ($n = m = 4$). The values of $\Delta H^0_{f(g)Cl^-}$ (363 kJ mol^{-1}) and $\Delta H^0_{f(g)BF_4^-}$ (−1687 kJ mol^{-1}) have been found in the database.[54] The rest energies have been obtained at the GGA/PBE/DND level of theory using the DMol^3 code.[45] As it follows from these calculations, the $\Delta H^0_{f(s)}$ value is higher by 1930 kJ mol^{-1} for **PDC** compared to **PDT**.

To calculate the energy released by the decomposition of **PDC** and **PDT** one should take into account the detonation products.[55] According to the H_2O—CO_2 arbitrary, the decomposition reactions for the studied diazonium salts can be presented as the following (the experimental ΔH^0_f are taken from the database[54]):

$$C_6H_5N_2^+Cl^- \rightarrow 5C_{(gr)} + N_2 + CH_4 + HCl \quad \Delta H^0_f = -167 \text{ kJ mol}^{-1}$$

$$C_6H_5N_2^+BF_4^- \rightarrow 1/2B_2F_4 + 2HF + 21/4C_{(gr)} + N_2 + 3/4CH_4 \quad \Delta H^0_f = -1319 \text{ kJ mol}^{-1}$$

As it follows from these equations, the **PDT** products are more stable than the **PDC** products by 1152 kJ mol^{-1}. Taking into account that **PCD** and **PDT** contain 14 and 18 atoms, respectively, the energy content (E_d) is by 1000 kJ mol^{-1} larger for **PDC** with respect to the value for **PDT**. This conclusion is in the complete accord with the energy content approach.[27] This quantity can be considered as an additional descriptor of impact sensitivity for the studied crystalline aryl diazonium salts. It is worth noting that the enthalpies of sublimation are rather close for **PDC** and **PDT** (746 vs. 626 kJ mol^{-1}). Thus, the main reason of such different solid-state enthalpies is due to the gas-phase heats of formation of the anions.

4 | CONCLUSIONS

In summary, we have performed a comprehensive theoretical study of two crystalline phenyl diazonium salts, **PDC** and **PDT**, as probes for evaluation of the solid state properties, which can serve as criteria of impact sensitivity. In the presented work, we have calculated and analyzed crystal structure, electronic properties, vibrational spectra, elasticity, crystal growth morphology, and the solid-state enthalpies of formation. The obtained results clearly suggest that most of the obtained properties are rather close for the studied salts. Only two parameters were found to be different enough. The first of them determines the pressure value, which corresponds to a zero band gap (so-called metallization point) and the second quantity is the stored energy content. These two descriptors can be applied as criteria of impact sensitivity.

Indeed, the **PDC** crystal possesses a rather small metallization point (29 GPa), whilst the **PDT** crystal is extremely stable and demonstrates the value of 200 GPa. These results are in agreement with the experimental pattern of aryl diazonium salts sensitivity.[7] The results of theoretical analysis of the rest possible factors affecting impact sensitivity, namely, energy transfer probability, bulk modulus, crystal growth morphology, and so forth agree with the hypothesis about the role of filling of conduction bands in the decomposition process initialization. The role of low-lying excited states in impact sensitivity should be done in further theoretical studies. It is known that the nucleophilicity/electrophilicity parameters[56] as well as chemical reactivity of the aryl cations (former aryl diazonium cations fragments)[57] is very different in the excited singlet or triplet state. Thus, the analysis of electronic excitations at different pressures is very interesting and will be performed in upcoming work.

ACKNOWLEDGMENTS

This work was supported by the Ministry of Education and Science of Ukraine, Research Fund (Grant No. 0113U001694). We thank Professor Hans Ågren (KTH, Stockholm) for the PDC supercomputer use. The computations were performed on resources provided by the Swedish National Infrastructure for Computing (SNIC) at the Parallel Computer Center (PDC) through the project "Multiphysics Modeling of Molecular Materials," SNIC 020/11–23.

REFERENCES

[1] T. M. Klapötke, J. Stierstorfer, in *Green Energetic Materials* (Ed: T. Brinck), Weinheim: Wiley **2014**.

[2] T. M. Klapötke, in *High Energy Density Materials* (Ed: T. M. Klapötke), Springer-Verlag, Berlin **2007**.

[3] S. V. Bondarchuk, B. F. Minaev, *Phys. Chem. Chem. Phys.* **2017**, *19*, 6698.

[4] S. V. Bondarchuk, B. F. Minaev, *Comput. Mater. Sci.* **2017**, *133*, 122.

[5] M. I. Eremets, A. G. Gavriliuk, I. A. Trojan, D. A. Dzivenko, R. Boehler, *Nat. Mater.* **2004**, *3*, 558.

[6] R. Matyáš, J. Pachman, in *Primary Explosives*, Springer-Verlag, Berlin **2013**.

[7] R. Ullrich, T. Grewer, *Thermochim. Acta* **1993**, *225*, 201.

[8] J. Sharma, B. C. Beard, M. Chaykovsky, *J. Phys. Chem.* **1991**, *95*, 1209.

[9] W.-L. Yan, S. Zeman, *Int. J. Quantum Chem.* **2013**, *113*, 1049.

[10] L. Türker, *J. Energ. Mater.* **2009**, *27*, 94.

[11] M. H. Keshavarz, Z. Keshavarz, *Z. Anorg. Allg. Chem.* **2016**, *642*, 335.

[12] M. Vaullerin, A. Espagnacq, L. Morin-Allory, *Prop. Explos. Pyrotech.* **1998**, *23*, 237.

[13] M. H. Keshavarz, *Prop. Explos. Pyrotech.* **2013**, *38*, 754.

[14] R. Wang, J. Jiang, Y. Pan, *J. Energ. Mater.* **2012**, *30*, 135.

[15] D. Mathieu, T. Alaime, *J. Mol. Graph. Model.* **2015**, *62*, 81.

[16] Z.-X. Chen, H.-M. Xiao, *Prop. Explos. Pyrotech.* **2014**, *39*, 487.

[17] P. Politzer, P. Lane, J. S. Murray, *Mol. Phys.* **2016**, *1*,

[18] H. Nefati, J.-M. Cense, J.-J. Legendre, *J. Chem. Inf. Comput. Sci.* **1996**, *36*, 804.

[19] D. I. A. Millar, I. D. H. Oswald, D. J. Francis, W. J. Marshall, C. R. Pulham, A. S. Cumming, *Chem. Commun.* **2009**, *562*.

[20] A. J. Davidson, I. D. H. Oswald, D. J. Francis, A. R. Lennie, W. J. Marshall, D. I. A. Millar, C. R. Pulham, J. E. Warren, A. S. Cumming, *CrystEngComm* **2008**, *10*, 162.

[21] Q. Peng, Rahul, G. Wang, G.-R. Liu, S. De, *Phys. Chem. Chem. Phys.* **2014**, *16*, 19972.

[22] H. Zhang, F. Cheung, F. Zhao, X.-L. Cheng, *Int. J. Quantum Chem.* **2009**, *109*, 1547.

[23] W. Zhu, H. Xiao, *Struct. Chem.* **2010**, *21*, 657.

[24] K. L. McNesby, C. S. Coffey, *J. Phys. Chem. B* **1997**, *101*, 3097.

[25] S. V. Bondarchuk, B. F. Minaev, *RSC Adv.* **2015**, *5*, 11558.

[26] Y. Ma, A. Zhang, X. Xue, D. Jiang, Y. Zhu, C. Zhang, *Cryst. Growth Des.* **2014**, *14*, 6101.

[27] L. E. Fried, M. R. Manaa, P. F. Pagoria, R. L. Simpson, *Annu. Rev. Mater. Res.* **2001**, *31*, 291.

[28] P. Politzer, J. S. Murray, *J. Mol. Model.* **2015**, *21*, 262.

[29] D. Mathieu, *Ind. Eng. Chem. Res.* **2016**, *55*, 7569.

[30] E. P. Koval'chuk, O. V. Reshetnyak, Z. Ye. Kozlovs'ka, J. Błażejowski, R. E. Gladyshevs'kyj, M. D. Obushak, *Thermochim. Acta* **2006**, *444*, 1.

[31] A. E. Fogel'zang, V. Ya. Adzhemyan, B. S. Svetlov, *Combust. Explos. Shock Waves* **1974**, *10*, 392.

[32] B. F. Minaev, S. V. Bondarchuk, M. A. Gîrţu, *J. Mol. Struct. THEOCHEM* **2009**, *904*, 14.

[33] S. V. Bondarchuk, B. F. Minaev, *J. Mol. Struct. THEOCHEM* **2010**, *952*, 1.

[34] C. Römming, *Acta Chem. Scand.* **1963**, *17*, 1444.

[35] M. Cygler, M. Przybylska, R. Elofson, *Can. J. Chem.* **1982**, *60*, 2852.

[36] U. Müller, A. Utterodt, W. Mörke, B. Deubzer, C. Herzig, *J. Photochem. Photobiol. A* **2001**, *140*, 53.

[37] M. Sheng, D. Frurip, D. Gorman, *J. Loss Prevent. Proc.* **2015**, *38*, 114.

[38] V. D. Filimonov, M. Trusova, P. Postnikov, E. A. Krasnokutskaya, Y. M. Lee, H. Y. Hwang, H. Kim, K.-W. Chi, *Org. Lett.* **2008**, *10*, 3961.

[39] K. V. Kutonova, M. E. Trusova, P. S. Postnikov, V. D. Filimonov, J. Parello, *Synthesis* **2013**, *45*, 2706.

[40] *Materials Studio 7.0*, Accelrys, Inc., San Diego, CA **2013**.

[41] S. J. Clark, M. D. Segall, C. J. Pickard, P. J. Hasnip, M. J. Probert, K. Refson, M. C. Payne, *Z. Kristallogr.* **2005**, *220*, 567.

[42] J. P. Perdew, K. Burke, M. Ernzerhof, *Phys. Rev. Lett.* **1996**, *77*, 3865.

[43] A. Tkatchenko, M. Scheffler, *Phys. Rev. Lett.* **2009**, *102*, 073005.

[44] B. Delley, *J. Chem. Phys.* **2000**, *113*, 7756.

[45] B. Delley, *J. Chem. Phys.* **1990**, *92*, 508.

[46] H. Sun, *J. Phys. Chem. B* **1998**, *102*, 7338.

[47] Z. Berkovitch-Yellin, *J. Am. Chem. Soc.* **1985**, *107*, 8239.

[48] W. Setyawan, S. Curtarolo, *Comput. Mater. Sci.* **2010**, *49*, 299.

[49] S. Curtarolo, W. Setyawan, G. L. W. Hart, M. Jahnatek, R. V. Chepulskii, R. H. Taylor, S. Wang, J. Xue, K. Yang, O. Levy, M. J. Mehl, H. T. Stokes, D. O. Demchenko, D. Morgan, *Comput. Mater. Sci.* **2012**, *58*, 218.

[50] B. F. Minaev, S. V. Bondarchuk, A. Y. Fesak, *Russ. J. Appl. Chem.* **2010**, *83*, 36.

[51] J. F. Nye, *Physical Properties of Crystals*, Oxford University Press Inc, Oxford **1985**.

[52] Q. An, T. Cheng, W. A. Goddard III, S. V. Zybin, *J. Phys. Chem. C* **2015**, *119*, 2196.

[53] M. R. Manaa, I.-F. W. Kuo, L. E. Fried, *J. Chem. Phys.* **2014**, *141*, 064702.

[54] S. G. Lias, J. E. Bartmess, J. F. Liebman, J. L. Holmes, R. D. Levin, W. G. Mallard, *J. Phys. Chem. Ref. Data* **1988**, *17*, 872.

[55] D. Mathieu, T. Alaime, *J. Phys. Chem. A* **2014**, *118*, 9720.

[56] S. V. Bondarchuk, B. F. Minaev, *Chem. Phys. Lett.* **2014**, *607*, 75.

[57] S. V. Bondarchuk, B. F. Minaev, A. Yu, Fesak, *Int. J. Quantum Chem.* **2013**, *113*, 2580.

SUPPORTING INFORMATION

Additional Supporting Information may be found online in the supporting information tab for this article.

How to cite this article: Bondarchuk SV. Impact sensitivity of crystalline phenyl diazonium salts: A first-principles study of solid-state properties determining the phenomenon. *Int J Quantum Chem*. 2017;e25430. https://doi.org/10.1002/qua.25430